Eur. Phys. J. B **49**, 325–331 (2006)
DOI: 10.1140/epjb/e2006-00074-4

THE EUROPEAN PHYSICAL JOURNAL B

Phonon effects in tunnelling through a double quantum dot molecule

Xin Lu, Jing Wang, and Chang-Qin Wu[a]

Department of Physics, Fudan University, Shanghai 200433, P.R. China

Received 27 September 2005
Published online 10 March 2006 –

Abstract. Phonon effects in tunnelling through a double quantum dot molecule are investigated by use of a recently developed technique, which is based on an exact mapping of a many-body electron-phonon interaction problem onto a multichannel one-body problem. The molecule is sandwiched between two ideal electrodes and the electron at each dot of the molecule interacts independently with Einstein phonons. Single-electron transmission rates through the molecule are computed and the nonlinear spectrum obtained shows a structure with many more satellite peaks due to the excitations of phonons. The strength of resonant peaks is found to be strongly dependent on the number of excited phonons. The effects of electron-phonon interaction on the current and shot noise, depending on the voltage bias applied at the two electrodes as well as the potential energy of the molecule, are discussed.

PACS. 71.38.+k Polarons and electron-phonon interactions – 73.23.Hk Coulomb blockade; single-electron tunneling – 73.50.Bk General theory, scattering mechanisms – 03.65.-w Quantum mechanics

1 Introduction

In recent years, modern advanced nanotechnology and progress in molecular electronics have made it possible to design and fabricate single-molecule devices, which has renewed interest in tunnelling through a mesoscopic system with electron-electron and/or electron-phonon interactions. A molecular device exhibiting switching behavior with large on-off ratios is an example [1]. Although the mechanism of the electron conduction on such a single-molecule device is not well understood yet, a series of experiments were reported [1–6], that suggest the quantum nature of transport properties have been observed, some of which suggest that vibrational modes play a role in transport processes [5,6]. Particularly, inelastic scattering effects have been observed directly in scanning tunnelling microscopy (STM) of the differential conductance of a molecule absorbed on metallic substrates [7–9]. The importance of coupling between electron and phonon in double quantum dot systems has been demonstrated [10,11]. For example, for freely suspended quantum dot cavities conductance near zero bias is completely suppressed as single electron tunnelling produces the excitation of a discrete cavity phonon [12]. Besides the experimental work, there are also lots of theoretical investigations on electronic tunnelling through molecules, in which the electron-phonon interaction is considered [13–25]. Among those works, some were based on ab initio [13–15] or semi-empirical methods [16–18], and some made use of various models to treat the tunneling problems in terms of the nonequilibrium Green's function techniques [19–22], the Fermi golden rule [23], and the Kinetic-equation approach [24,25].

For inelastic scattering processes with the emission and/or absorption of a phonon, the many-body problem involving electron states and various excited phonon states of the system, which consists of a mesoscopic conductor coupled with phonon modes as well as two single-channel ideal leads (acting as the electron source and drain respectively) attached to its two ends, can be mapped onto an exactly solvable multichannel single-electron scattering problem according to the work by Bonca and Trugman [26]. In the light of this technique, some theoretical investigations of phonon effects in electron tunnelling through some electron-phonon interacting systems have been reported [26–34], where the electron-phonon interaction is described either by the Holstein model [35] (where the electrons are coupled with an Einstein phonon mode at each site) or by the Su-Schreiffer-Heeger (SSH) model [36] (where the electrons are coupled with the phonon modes on bonds).

In this work we study a double quantum dot molecule sandwiched between two ideal leads. In the molecule,

[a] e-mail: cqw@fudan.edu.cn

each dot has a single electronic level at which the electron interacts with an associated Einstein phonon mode. We use the above mentioned mapping technique [26] to investigate the inelastic electron tunnelling through the electron-phonon interacting molecule by computing the single-electron transmission rates. The nonlinear spectrum obtained shows a structure with many more satellite peaks due to the excitations of phonons. The effects of electron-phonon interaction on the current and shot noise, depending on the voltage bias applied at the two electrodes as well as the potential energy of the molecule, are discussed.

The rest of this paper is organized as follows. In Section 2 we introduce the Hamiltonian for the tunnelling through the molecule and describe the theoretical method adopted in this work. In Section 3, we give the numerical results from the calculation within the framework given in Section 2. Finally, a summary is presented in the last section.

2 Model and method

The Hamiltonian H of the system we consider in this work can be written as follows:

$$H = H_M + H^L_{lead} + H^R_{lead} + H^L_{int} + H^R_{int}, \tag{1}$$

where

$$H_M = \sum_{i=1}^{2}(\epsilon_0 c_i^\dagger c_i + \omega_0 b_i^\dagger b_i) - t(c_1^\dagger c_2 + c_2^\dagger c_1) + \lambda \sum_{i=1}^{2}(b_i^\dagger + b_i)c_i^\dagger c_i \tag{2}$$

describes the double quantum dot molecule, in which each dot has a single electronic level (with energy ϵ_0) and the electron at the level couples with an Einstein phonon mode (with the same phonon frequency ω_0), $c_l^\dagger(c_l)$ denotes the electron creation (annihilation) operator on site i and $b_i^\dagger(b_i)$ for the phonon modes ($i = 1, 2$), t is the hopping constant between the two dots and λ is the coupling between the electron and phonon at the same site. At the two ends of the molecule, the ideal leads are considered as a chain of metallic atoms, then the Hamiltonians for the left and right leads are given as:

$$H^L_{lead} = \epsilon_+ \sum_{l=-\infty}^{0} c_l^\dagger c_l - t_0 \sum_{l=-\infty}^{-1}(c_l^\dagger c_{l+1} + \text{h.c}), \tag{3}$$

$$H^R_{lead} = \epsilon_- \sum_{l=3}^{\infty} c_l^\dagger c_l - t_0 \sum_{l=3}^{\infty}(c_l^\dagger c_{l+1} + \text{h.c}), \tag{4}$$

where the potentials $\epsilon_\pm$ at the left (right) lead are given by $\epsilon_\pm = \pm eV/2$, V is the voltage bias applied at the left and right lead and e the absolute value of electron charge. The electrons in the metallic leads hop from one site to its nearest-neighbor site with the hopping parameter t_0. The coupling between the molecule and the leads are described simply by

$$H^L_{int} = -\Gamma(c_0^\dagger c_1 + c_1^\dagger c_0), \tag{5}$$

$$H^R_{int} = -\Gamma(c_2^\dagger c_3 + c_3^\dagger c_2), \tag{6}$$

where Γ is the coupling strength between the molecule and its associated leads.

Following the technique [26] that maps a many-body problem onto a multichannel one-body problem, we consider an incident electron moving through the molecule from the left lead to the right lead by solving exactly the Schrödinger equation $H\psi = E\psi$. An incident electron enters into the left lead at one of the channels, such as channel n, then it elastically or inelastically goes into the right lead at one time at the channel n', where n and n' could be taken as the number of excited phonons before and after the scattering. Now we can write down the wave function for the electron as

$$|\psi\rangle^n = |\psi\rangle^n_L + |\psi\rangle^n_M + |\psi\rangle^n_R, \tag{7}$$

where

$$|\psi\rangle^{(n)}_L = \sum_{j=-\infty}^{0} e^{ik^n j}|j\rangle \otimes |n\rangle + \sum_{n'} r_{n,n'} \sum_{j=-\infty}^{0} e^{ik^{n'} j}|j\rangle \otimes |n'\rangle \tag{8}$$

describes the incident electron and the reflection from the molecule,

$$|\psi\rangle^{(n)}_M = \sum_{n'}\sum_{j=1}^{2} u_j^{n,n'}|j\rangle \otimes |n'\rangle \tag{9}$$

gives the wave function at the molecule, and

$$|\psi\rangle^{(n)}_R = \sum_{n'} t_{n,n'} \sum_{j=3}^{\infty} e^{ik^{n'} j}|j\rangle \otimes |n'\rangle \tag{10}$$

are the wave function of the outgoing electron at the right lead. In those wave functions, $|j\rangle$ indicates an electron occupying the j-th site and $|n\rangle$ is a phonon state of the molecule with the total number of phonons as n, $r_{n,n'}$ and $t_{n,n'}$ represent the reflection and transmission amplitudes. The incident wave vector k^n and reflecting (outgoing) wave vector $k^{n'}$ are restricted by the energy conservation

$$\epsilon_+ - 2t_0\cos(k^n) + n\omega = \epsilon_\pm - 2t_0\cos(k^{n'}) + n'\omega, \tag{11}$$

which is the eigen-energy E in the Schrödinger equation. Now we can obtain $r_{n,n'}$ and $t_{n,n'}$ by solving the Schrödinger equation self-consistently, the maximum number of phonons N_{ph} is taken as large as the result reaches convergence.

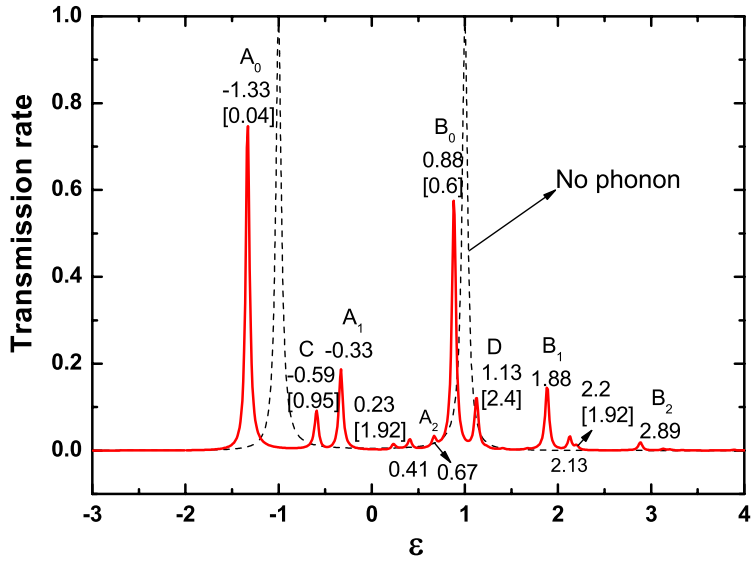

Fig. 1. Total transmission rate as a function of the incident electron energy at zero temperature. The solid line is for the molecule with the e-p interaction while the dashed line is for that without phonons. The numbers above peaks give the value of incident energies while that in square brackets gives the mean number of excited phonons. The model parameters are taken as $\lambda = 0.7, \omega_0 = 1.0, \epsilon_0 = 0$, $V = 0$, and $\Gamma = 0.5$.

With the transmission and reflection amplitudes for each scattering channel we have the elements of transmission and reflection matrices as[29]

$$T^{(n,n')}(\epsilon,\epsilon') = |t_{n,n'}|^2 \frac{\sin k_R^{n'}}{\sin k_L^{n}}, \tag{12}$$

$$R^{(n,n')}(\epsilon,\epsilon') = |r_{n,n'}|^2 \frac{\sin k_L^{n'}}{\sin k_L^{n}}, \tag{13}$$

where ϵ (ϵ') represents the incoming (outgoing) electron energies, i.e., $\epsilon \equiv -2t_0\cos(k^n)$ and $\epsilon' \equiv -2t_0\cos(k^{n'})$. The total transmission rate should be a sum of those single-channel rates over all incoming channels n weighted by the probability $P(n) = P(n_1)P(n_2)$ with $P(n_i) = (1 - e^{-\beta\omega_0})e^{-n_i\beta\omega_0}$ $(i = 1, 2)$ and all outgoing channels n'

$$T(\epsilon) = \sum_{n,n'} P(n) T^{(n,n')}(\epsilon,\epsilon'). \tag{14}$$

For the case when a finite bias voltage is applied to the molecule, the one-electron approximation can be adopted in the calculation of the total electronic current through the molecule, which can be measured experimentally,

$$I = \frac{e}{h}\int d\epsilon \sum_{n,n'} T^{(n,n')}(\epsilon,\epsilon') \left[P(n) f_L(\epsilon)\left(1 - f_R(\epsilon')\right) - P(n') f_R(\epsilon')\left(1 - f_L(\epsilon)\right)\right], \tag{15}$$

where f_L and f_R are the electron Fermi distribution functions for the left and right leads, respectively. Furthermore, from scattering theory, the total shot noise of the current through the double dot molecule is given by [34,37,38]

$$\begin{aligned} S = &\frac{2e^2}{h}\int d\epsilon \sum_{n,n'} T^{(n,n')}(\epsilon,\epsilon') \\ &\times \Big\{ T^{(n,n')}(\epsilon,\epsilon')\big\{P(n) f_L(\epsilon)\left[1 - f_L(\epsilon')\right] \\ &+ P(n') f_R(\epsilon')\left[1 - f_R(\epsilon)\right]\Big\} \\ &+ R^{(n,n')}(\epsilon,\epsilon')\big\{P(n) f_L(\epsilon)\left[1 - f_R(\epsilon')\right] \\ &+ P(n') f_R(\epsilon')\left[1 - f_L(\epsilon)\right]\big\}\Big\}. \end{aligned} \tag{16}$$

The summation over the outgoing channels n' indicates that we have included contributions from both the elastic and inelastic scattering. By restricting $n' = n$, we can obtain those quantities contributed only by the elastic transmission. Finally in the end of this section we give the definition of the Fano factor [34,37,38]:

$$F = \frac{S}{2eI}. \tag{17}$$

3 Numerical results

In this section we present the numerical results on the transmission rates, currents and shot noise together with the analysis on the effects of electron-phonon interactions. We will take $t = 1$, i.e., the unit of energies is taken as t, the hopping constant between the two dots in the molecule. Furthermore, we consider the leads having an energy band that is almost flat in the vicinity of Fermi points, for which we take $t_0 = 10$, a large enough value in the calculations.

3.1 Transmission

First of all we show the total transmission rate as a function of the incidence electron energy ϵ at zero temperature in Figure 1. It is clear that the molecule contains no phonons before the electron tunnelling, so only phonon

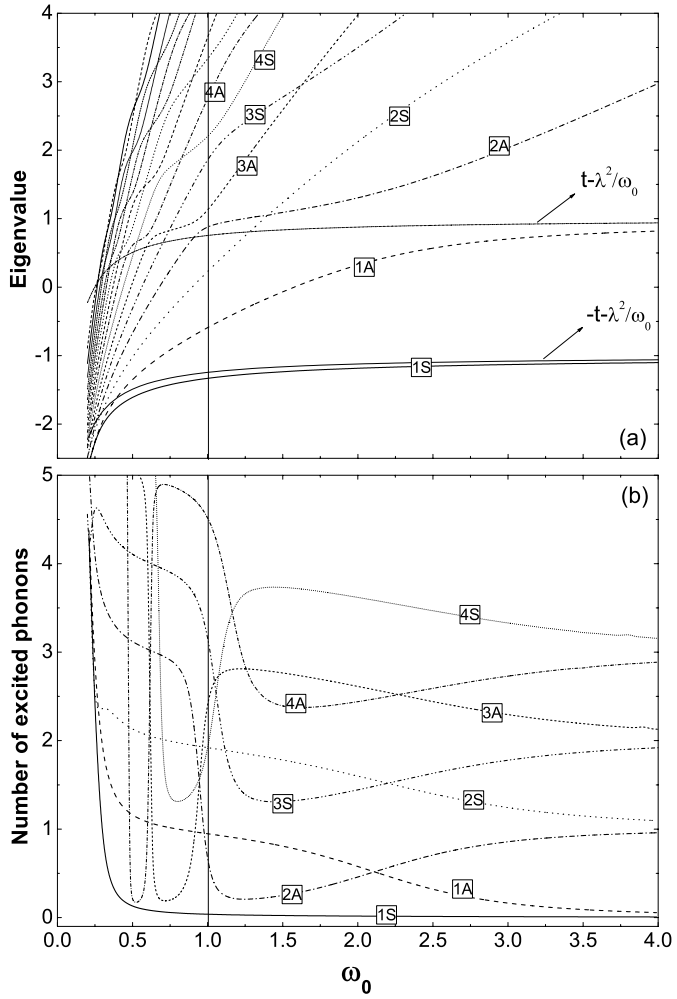

Fig. 2. (a) The eigenvalues of the transformed Hamiltonian H_1 for the molecule as functions of the phonon frequency ω_0. The sign S (A) indicates the states being symmetric (antisymmetric). (b) The mean number of excited phonons at corresponding eigenstates. $\lambda = 0.7$.

emission processes are allowed at zero temperature. In the absence of electron phonon interaction there are two peaks that appear in the transmission spectrum, they should be corresponding to the resonant energy levels $\epsilon_0 \pm t$ ($\epsilon_0 = 0$ in Fig. 1), which are the bonding and anti-bonding states in the molecule. In the presence of the coupling between the electron and phonon, these two peaks are shifted and many side peaks can been seen in the spectrum which should indicate many more resonant states exist in the molecule now.

To understand the origin of those states, we make a transformation on the molecule Hamiltonian and decouple it into two parts H_1 and H_2 (see Appendix A). While H_2 gives the spectra $n\omega_0$ of free phonons, H_1 can be diagonalized by a numerical method, the results are shown in Figure 2. Due to the symmetry of the two dots exchange, the eigenstates are either symmetric or antisymmetric, we use S and A to indicate these states' symmetries in the figure. It is clear that there is only level crossing between S and A states. No crossing occurs for states of the same symmetry. It should be very easy to expect that at anti-adiabatic limit ($\omega_0 \to \infty$), the lowest two states of H_1 should have energies $\pm t - \lambda^2/\omega_0$, which should evolve from the bonding and anti-bonding states in the absence of the e-p interaction. But from Figure 2a, we see it is not true. At $\omega_0 = 1$, the $2A$ state is closest to the line $t - \lambda^2/\omega_0$ while the $1S$ is always closest to the line $-t - \lambda^2/\omega_0$. This fact indicates that the most weighted two peaks in the transmission spectrum (solid line in Fig. 1) are not simply evolved from the two peaks in the absence of the e-p interaction (dashed line in Fig. 1). The first one (indicated by A_0) is caused by the $1S$ state, which is evolved from the bonding state. With the contribution of H_2, we identify the peak A_1 and A_2, which correspond to the $1S$ state with one and two more excited-phonons (d_1 mode). It is clear that the energy of the resonant peak A_n is $\epsilon(A_n) = \epsilon_0 - t - \lambda^2/\omega_0 + n\omega_0$. The resonant strength is decreased with the increase of the excited-phonon number. Figure 2b shows the mean number of excited phonons $\langle d_2^\dagger d_2 \rangle$ at corresponding eigenstates of H_1. The resonant peak B_0 in Figure 1 is due to the $2A$ state, which has a lower value of excited phonons than that in the $1A$ state. Similarly, we identify B_1 and B_2 together with B_0 as the first three peaks in the series of B_n of the energy $\epsilon(B_n) = \epsilon_0 + t - \lambda^2/\omega_0 + n\omega_0$. The peaks A_n or B_n represent the processes accompanying with emission of n bare phonons. The peak C at $\epsilon = -0.59$ is due to the $1A$ state of the number of excited phonons 0.95. A very interesting fact is that the strength of resonant peaks in the transmission spectra is strongly dependent on the mean number of excited phonons at the corresponding states, i.e., the strength of the resonant transmission decreases with the increase of the number of excited phonons. An exception is the peak D at $\epsilon = 1.13$, which is clearly due to the $3A$ state of the number of excited phonons 2.4, the strength of the peak D is larger than that of the peak C. This exception may be caused by the mixing of the $2A$ and $3A$ states due to the coupling between the leads and molecule. We will see later that the exception will not appear at Figure 3 with other value of ω_0 where the two states are not closed again.

From Figure 3, we see that the first resonant peak A_0 due to the $1S$ state as well as other peaks in the series of A_n stand almost unchanged with different values of the phonon frequency ω_0. But the resonant peak B_0 as well as other peaks in the series of B_n are changed significantly and B_0 is caused by the $4A$, $3A$, $2A$, and $1A$ states , respectively, with the increase of the phonon frequency ω_0 from 0.52 to 3.0 in Figure 3. We can see the resonant peak C is caused by the $1A$ state in Figures 3a–3c while the peak C is just the B_0 in Figure 3d. For those cases, we see the fact the higher resonant peaks correspond to the states with a smaller number of excited phonons without exception.

3.2 Current and shot noise

We now present the calculated current and shot noise for the system. In Figure 4, we plot the currents (a) and shot

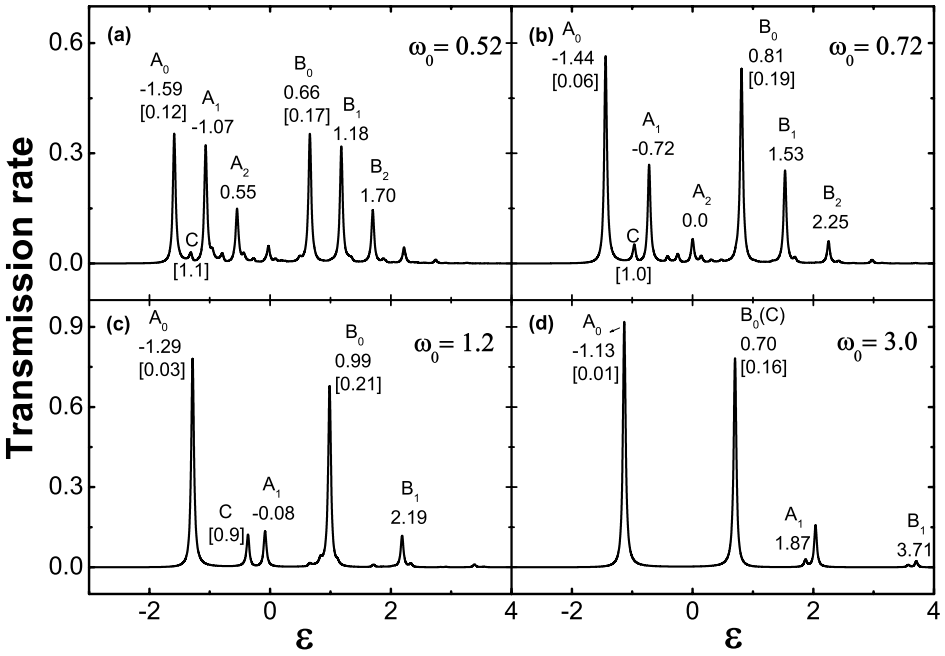

Fig. 3. The same as in Figure 1 but for for different phonon frequency ω_0.

noises (b) as functions of the bias voltage V between the two leads. In comparison, we also draw the current and shot noise in the absence of the electron-phonon interaction in Figure 4c. Comparing Figure 4a and 4b, we find that along with the increasing bias voltage V, the current and shot noise show similar varying characteristics. Without regard to coupling between electrons and phonons, the step structures in Figure 4c only rest on the molecule's potential energy ϵ_0, the position of peaks in differential conductance dI/dV and differential shot noise dS/dV (thin lines in Fig. 4d) correspond to the condition $V = \epsilon_+ - \epsilon_- = 2t$. However, many more steps appear in the current and shot noise once the electron phonon interaction is turned on. In correspondence with these new steps more resonant peaks in differential current and differential shot noise (thick lines in Fig. 4d) are presented due to the contributions of the phonon emission (and the absorption at non-zero temperature), which implies new opened pseudo-channels have contributed to the tunnelling process. Actually, these characters have already been seen in Figure 1. By looking into the graph of differential shot noise, we can find a sunken shape in the absence of the electron phonon interaction. In the expression of shot noise, this contains $[T(1-T)]$ [38], which means that the expression has an extremum if T is big enough. However, no sunken shape appears in Figure 4d in the presence of the electron phonon interaction, since the transmission rate is reduced significantly by the interaction. As long as the *e-ph* coupling is weak enough or the phonon frequency is very large, the shape will appear again in the differential shot noise.

As the definition in equation (17), the Fano factor F is the ratio of actual shot noise and the Poisson noise that would be measured if the system produced the noise due to single independent electrons [37]. It is clear that neither closed ($T^n = 0, F = 1$) nor open ($T^n = 1, F = 0$) channels contribute to shot noise, the maximal contribution to shot noise comes from channels with $T^n = 1/2$ [37]. Figure 5 presents the bias-dependent Fano factor for the molecule system. In the absence of the electron phonon interaction, the Fano factor shows a very simple structure since the Fermi surface is at the middle of two resonant energy levels in the double dot molecule. The electron-phonon interaction results in an enhancement and more fine structures in the Fano factor.

4 Summary

In summary, we have extended a numerical method to exactly resolve the tunnelling process through a double quantum dot molecule (a multi-dot problem could be treated in the same way) by mapping a many-body electron phonon interaction problem onto a multichannel single electron scattering problem. The result shows that, this tunnelling process through the double dot molecule can not be understood simply as the addition of two independent tunnelling processes through a single dot molecule due to the complex energy-level structure of the molecule. Since the approach is entirely based on a one-electron approximation, the result presented here would be realized only for a finite applied bias voltage, which is fortunately at the range of interests for applications. Even though the results are obtained on the basis of a zero-temperature calculation, they can easily be generalized to cases at any finite temperatures. Single-electron

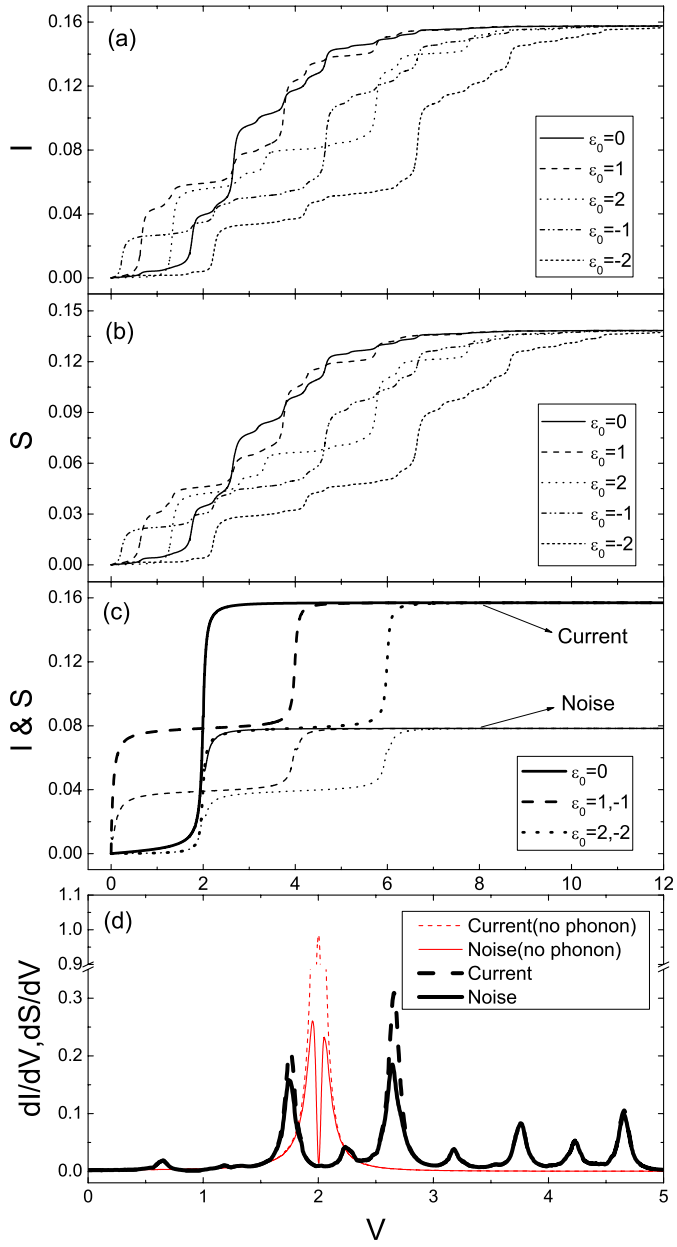

Fig. 4. The calculated current I and shot noise S as functions of the bias voltage V in the presence (a, b) and absence (c) of the e-p interaction for various energies ϵ_0 on the molecule. (d) The differential conductance dI/dV (dashed line) and differential shot noise dS/dV (solid line) at $\epsilon_0 = 0$ in the presence (thick lines) and absence (thin lines) of the e-p interaction. All parameters but the voltage bias are taken to be the same as that in Figure 1.

transmission rates through the molecule shows a structure of many more satellite peaks due to the excitations of phonons. The strength of resonant peaks is found to be strongly dependent on the number of excited phonons. The effects of electron-phonon interaction on the current and shot noise, depending on the voltage bias applied at the two electrodes as well as the potential energy of the molecule, are discussed.

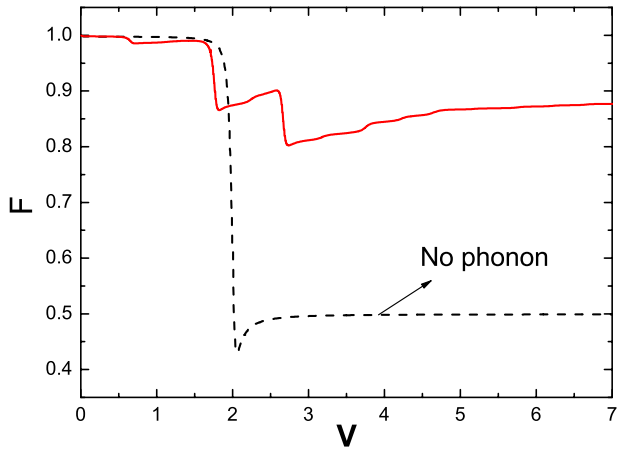

Fig. 5. Fano factor as a function of the voltage bias V with (solid line) and without (dashed line) electron phonon interaction. The parameters are the same as in Figure 1.

This work was supported by the National Natural Science Foundation of China (Nos. 90403110, 10374017, and 10321003) and the State Ministry of Education of China (No. 20020246006).

Appendix A: Exact solution of the double quantum dot molecule

To get the exact solution of the double quantum dot molecule, H_M in equation (2), we first consider the symmetry of the two dots, i.e., we make transformation on the both of electron and phonon operators,

$$\begin{aligned} c_1 &= \frac{1}{\sqrt{2}}(a_1 + a_2), \quad c_2 = \frac{1}{\sqrt{2}}(a_1 - a_2), \\ b_1 &= \frac{1}{\sqrt{2}}(d_1 + d_2), \quad b_2 = \frac{1}{\sqrt{2}}(d_1 - d_2), \end{aligned} \tag{A.1}$$

the Hamiltonian H_M becomes

$$\begin{aligned} H_M = &(\epsilon_0 - t)a_1^\dagger a_1 + \frac{\lambda}{\sqrt{2}}(d_1^\dagger + d_1)a_1^\dagger a_1 + \omega_0 d_1^\dagger d_1 \\ &+(\epsilon_0 + t)a_2^\dagger a_2 + \frac{\lambda}{\sqrt{2}}(d_1^\dagger + d_1)a_2^\dagger a_2 \\ &+\frac{\lambda}{\sqrt{2}}(d_2^\dagger + d_2)(a_1^\dagger a_2 + a_2^\dagger a_1) + \omega_0 d_2^\dagger d_2, \end{aligned} \tag{A.2}$$

where a_1 and d_1 are symmetric while a_2 and d_2 are antisymmetric. Now we can see that the first two lines in the above Hamiltonian show two separated dots each coupled with a phonon mode, which can be diagonalized through a canonical transformation [21,39] while the third line in the above equation will not be changed if we use the same operators for renormalized ones, the resultant Hamiltonian can be written as two decoupled parts:

$$\bar{H}_M = H_1 + H_2, \tag{A.3}$$

where

$$H_1 = (\epsilon_0 - t - \frac{\lambda^2}{2\omega_0})a_1^\dagger a_1 + (\epsilon_0 + t - \frac{\lambda^2}{2\omega_0})a_2^\dagger a_2 + \frac{\lambda}{\sqrt{2}}(d_2^\dagger + d_2)(a_1^\dagger a_2 + a_2^\dagger a_1) + \omega_0 d_2^\dagger d_2, \quad \text{(A.4)}$$

$$H_2 = \omega_0 d_1^\dagger d_1. \quad \text{(A.5)}$$

For H_1, we can make a numerical diagonalization to obtain all eigen-states while H_2 gives the bare phonon spectra $n\omega_0$ with n all non-negative integers as in the single quantum dot case where a similar part exists [21].

References

1. J. Chen, M.A. Reed, A.M. Rawlett, J.M. Tour, Science **286**, 1550 (1999)
2. M.A. Reed, C. Zhou, C.J. Muller, T.P. Burgin, J.M. Tour, Science **278**, 252 (1997)
3. D. Porath, A. Bezryadin, S. de Vries, C. Dekker, Nature (London) **403**, 635 (2000)
4. W. Liang, M.P. Shores, M. Bockrath, J.R. Long, H. Park, Nature (London) **417**, 725 (2002)
5. H. Park, J. Park, A.K.L. Lim, E.H. Anderson, A.P. Alivisatos, P.L. McEuen, Nature (London) **407**, 57 (2000)
6. N.B. Zhitenev, H. Meng, Z. Bao, Phys. Rev. Lett. **88**, 226801 (2002)
7. B.C. Stipe et al., Phys. Rev. Lett. **78**, 4410 (1997)
8. B.C. Stipe, M.A. Rezaei, W. Ho, Phys. Rev. Lett. **81**, 1263 (1998)
9. B.C. Stipe, M.A. Rezaei, W. Ho, Science **280**, 1732 (1998)
10. T. Fujisawa et al., Science **282**, 932 (1998); Physica E **7**, 413 (2000)
11. H. Qin, A.W. Holleitner, K. Eberl, R.H. Blick, Phys. Rev. B **64**, 241302 (2001)
12. E.M. Weig et al., Phys. Rev. Lett. **92**, 046804 (2004)
13. M. Di Ventra, S.T. Pantelides, N.D. Lang, Phys. Rev. Lett. **84**, 979 (2000)
14. J. Taylor, H. Guo, J. Wang, Phys. Rev. B **63**, 245407 (2001).
15. J.J. Palacios, A.J. Perez-Jimenez, E. Louis, J.A. Verges, Phys. Rev. B **64**, 115411 (2001)
16. L.E. Hall, J.R. Reimers, N.S. Hush, K. Silverbrook, J. Chem. Phys. **112**, 1510 (2000)
17. M. Paulsson, S. Stafström, Phys. Rev. B **64**, 035416 (2001)
18. E.G. Emberly, G. Kirczenow, Phys. Rev. B **62**, 10451 (2000)
19. N.S. Wingreen, K.W. Jacobsen, J.W. Wilkins, Phys. Rev. Lett. **61**, 1396 (1988); N.S. Wingreen, K.W. Jacobsen, J.W. Wilkins, Phys. Rev. B **40**, 11834 (1989)
20. U. Lundin, R. McKenzie, Phys. Rev. B **66**, 075303 (2002)
21. J.X. Zhu, A.V. Balatsky, Phys. Rev. B **67**, 165326 (2003)
22. K. Flensberg, Phys. Rev. B **68**, 205323 (2003); S. Braig, K. Flensberg, Phys. Rev. B **68**, 205324 (2003)
23. P.J. Turley, S.W. Teitsworth, Phys. Rev. B **44**, 3199 (1991)
24. T. Brandes, B. Kramer, Phys. Rev. Lett. **83**, 3021 (1999); T. Brandes, N. Lambert, Phys. Rev. B **67**, 125323 (2003)
25. D. Bose, H. Schöller, Europhys. Lett. **54**, 668 (2001)
26. J. Bonca, S.A. Trugman, Phys. Rev. Lett. **75**, 2566 (1995)
27. J. Bonca, S.A. Trugman, Phys. Rev. Lett. **79**, 4874 (1997)
28. H. Ness, A.J. Fisher, Phys. Rev. Lett. **83**, 452 (1999)
29. K. Haule, J. Bonca, Phys. Rev. B **59**, 13087 (1999)
30. E.G. Emberly, G. Kirczenow, Phys. Rev. B **61**, 5740 (2000)
31. H. Ness, S.A. Shevlin, A.J. Fisher, Phys. Rev. B **63**, 125422 (2001)
32. L.E.F. Foa Torres, H.M. Pastawski, S.S. Makler, Phys. Rev. B **64**, 193304 (2001)
33. M.I. Vasilevskiy, E.V. Anda, S.S. Makler, Phys. Rev. B **70**, 035318 (2004)
34. B. Dong, H.L. Cui, X.L. Lei, N.J.M. Horing, Phys. Rev. B **71**, 045331 (2005)
35. T. Holstein, Ann. Phys. (N.Y.S) **8**, 325 (1959); T. Holstein, Ann. Phys. (N.Y.S) **8**, 343 (1959)
36. W.P. Su, J.R. Schrieffer, A.J. Heeger, Phys. Rev. Lett. **42**, 1698 (1979)
37. Ya. M. Blanter, M. Büttiker, Phys. Rep. **336**, 1 (2000)
38. M.J.M. de Jong, C.W.J. Beenakker, Mesoscopic Electron Transport **345**, 225 (1997)
39. G.D. Mahan, *Many-Particle Physics* (Plenum Press, New York, 2000)